

Are Existing Road Design Guidelines Suitable for Autonomous Vehicles?

Yang Sun, Christopher M. Poskitt, and Jun Sun

Abstract—The emergence of Autonomous Vehicles (AVs) has spurred research into testing the resilience of their perception systems, i.e. to ensure they are not susceptible to making critical misjudgements. It is important that they are tested not only with respect to other vehicles on the road, but also those objects placed on the roadside. Trash bins, billboards, and greenery are all examples of such objects, typically placed according to guidelines that were developed for the human visual system, and which may not align perfectly with the needs of AVs. Existing tests, however, usually focus on adversarial objects with conspicuous shapes/patches, that are ultimately unrealistic given their unnatural appearances and the need for white box knowledge. In this work, we introduce a black box attack on the perception systems of AVs, in which the objective is to create realistic adversarial scenarios (i.e. satisfying road design guidelines) by manipulating the positions of common roadside objects, and without resorting to ‘unnatural’ adversarial patches. In particular, we propose *TrashFuzz*, a fuzzing algorithm to find scenarios in which the placement of these objects leads to substantial misperceptions by the AV—such as mistaking a traffic light’s colour—with overall the goal of causing it to violate traffic laws. To ensure the realism of these scenarios, they must satisfy several rules encoding regulatory guidelines about the placement of objects on public streets. We implemented and evaluated these attacks for the Apollo, finding that *TrashFuzz* induced it into violating 15 out of 24 different traffic laws.

Index Terms—Autonomous Driving System, Autonomous Vehicle, Testing, Security, Fuzzing.

1 INTRODUCTION

Autonomous Vehicles (AVs) are currently undergoing rapid and promising development. Notably, several Level-4 AVs—which do not require driver intervention—have been successfully deployed in real-world traffic scenarios [1], including Google Waymo [2], Baidu Apollo [3], and TuSimple [4]. This success has spurred research into testing the resilience of their perception systems, i.e. to ensure they are not susceptible to making critical misjudgements. It is important that they are tested not only with respect to vehicles and obstacles on the road, but also those objects placed to its side, which have the potential to affect the overall perception. Trash bins, billboards, and greenery are all examples of such objects, typically placed according to guidelines (e.g. [5], [6], [7], [8], [9], [10]) that were developed for the human visual system, and may not align perfectly with the requirements of AVs.

Existing tests and attacks, however, usually focus on adversarial objects with conspicuous shapes or patches that have the potential to be noticed by human observers (e.g. [11], [12], [13], [14], [15], [16]). For instance, the adversarial traffic cone in MSF-ADV [11] significantly deviates from the appearance of a regular traffic cone, rendering it as relatively easy for humans to identify as suspicious. Furthermore, the objectives of current attacks tend to be limited to goals such as “ignoring the object” [11] or “misjudging the position of the object” [13], [14], [15], [16]. While these objectives could occasionally result in safety-critical

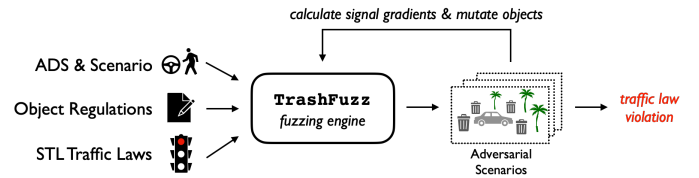


Fig. 1: TrashFuzz workflow: the fuzzer mutates the placement of roadside objects (e.g. trash bins, trees) so as to find ‘natural’ scenarios that induce the AV to violate traffic laws

situations, such as a high-speed collision with a traffic cone, the consequences of these misperceptions may be relatively benign with respect to the safety of the overall journey. Finally, these attacks generally require white box knowledge of the underlying models in the perception system, which is difficult to obtain in practice. Ultimately, these limitations make it challenging for existing attacks to be applied successfully on real roads.

These observations led us to consider two questions. First, to what extent can AV perception systems be deceived by objects that follow conventional road design guidelines and appear to humans as ‘natural’? In other words, is there a risk that certain placements of everyday (patch-free) roadside objects could accidentally (or intentionally) trigger a misperception by the AV? Second, if such a misperception occurs, is there a risk that it could lead to serious safety issues on the road, e.g. a collision, or even the violation of traffic laws [17]? If such scenarios are feasible—even if likely to be rare—then it is important to be able to demonstrate their presence in a testing tool before the AV encounters them on real roads.

- Y. Sun, C.M. Poskitt, J. Sun, are with the School of Computing and Information Systems, Singapore Management University, Singapore, 178902. E-mail: yangsun.2020@phdcs.smu.edu.sg, cposkitt@smu.edu.sg, jun-sun@smu.edu.sg.

To answer these questions, we developed a black box approach for systematically fuzzing the perception systems of AVs and uncovering scenarios in which their Autonomous Driving Systems (ADSs) are deceived into making dangerous manoeuvres. In particular, we generate scenarios consisting of ‘naturally’ placed, shaped, and patch-free roadside objects such as trash bins, benches, trees, and fire hydrants, then use a high-fidelity simulator to determine whether the scenario is able to cause the AV to violate basic safety properties and traffic laws. Our approach, called TrashFuzz, does not require any knowledge of how the AV and its perception system works; rather, it uses a greedy search algorithm to optimise the placement of objects and come ‘closer’ to violating signal temporal logic (STL) formulas expressing traffic laws. To ensure the realism of the generated scenarios, our algorithm is required to satisfy the constraints of various regulatory documents regarding the placement of roadside objects, including the ‘Code of Practice for Works on Public Streets’ [5], [6], the ‘Greenery Provision and Tree Conservation’ guidelines [7], as well as guidelines published by three prominent waste recycling companies, HDS, KIMBLE, and GRANGER [8], [9], [10]. Collectively, these guidelines establish a standard for the (otherwise subjective) ‘natural’ placement of everyday roadside objects such as fixed position boxes, trees, and trash bins. Figure 1 summarises the workflow of TrashFuzz.

We implemented TrashFuzz for a state-of-the-art ADS, Baidu Apollo (version 7.0 [18]), and the high-fidelity Unity-based LGSVL simulator [19]. We utilise the Unity Asset Store [20] to generate a diversity of everyday roadside objects within LGSVL, including trash bins in various shapes and colours, benches constructed with different materials, as well as fire hydrants, trees, and trash bags. TrashFuzz ensures these objects are placed according to rules extracted from the previously mentioned regulatory guidelines, then searches for scenarios in which the objects’ placement can trigger the AV to violate Signal Temporal Logic (STL)-based specifications of traffic laws. To evaluate the approach, we conducted a comprehensive comparative analysis against our fuzzing algorithm and found that TrashFuzz is efficient in generating scenarios that lead to various violations of the specifications. In addition, we found that 15 of the 24 traffic laws were violated by Apollo after solely manipulating the natural positions of roadside objects. Most of these attack scenarios induced hesitation in Apollo, causing it to fail to proceed. A few scenarios compelled Apollo to adopt a more aggressive driving behaviour, thereby significantly increasing the risk of potentially catastrophic accidents. This includes a scenario in which an otherwise benign placement of bins overloads Apollo’s perception system, causing it to perceive a red traffic light as green and illegally drive through it.

The overall results of this paper suggest that regulatory guidelines for the placement of objects on streets may need to consider the presence of AVs on the road, and that testing the resilience of AVs must also take into account anomalies arising from the placement of roadside objects.

The structure of this paper is organized as follows. In Section 2, we provide the necessary background information and define the attack goal, along with an introduction to our threat model. Section 3, we present our fuzzing algorithm.

We present the evaluation of our algorithm in Section 4. Lastly, we review related work in Section 5 and conclude in Section 6.

2 BACKGROUND AND PROBLEM

In this section, we review the design of state-of-the-art ADS perception systems, define the attack goal and threat model, the DSLs for specifying safety properties, and highlight the key design challenges our solution must address.

2.1 ADS Perception Systems

The perception systems of state-of-art ADSs such as Apollo [21], Autoware [22], and Waymo [2] have a number of common characteristics. These include the integration of multiple sensors and the utilisation of Deep Neural Networks (DNNs) for classification and segmentation tasks.

Integration of Multiple Sensors. The perception module assumes a pivotal role in ADSs. These advanced systems incorporate a multitude of sensors to improve the accuracy and resilience of perception. To the best of our knowledge, current Level-4 AVs, exemplified by Apollo [21] and Waymo [2], mandate a minimum of two distinct input sources for perception. This amalgamation of sensors, cameras, LiDAR, and radar, ensures ADSs are able to gather comprehensive and reliable information about their surrounding environments.

While this multi-sensor approach significantly improves an ADS’ perception ability, it does not guarantee its resilience in all circumstances. One example is MSF-ADV [11], which demonstrates the ability to create invisible adversarial objects that deceive both the camera and LiDAR detection algorithm.

DNN-based classification/segmentation. DNNs have a distinct advantage at processing data that can be represented as vectors. They are effective at learning complex patterns and relationships within high-dimensional data, and thus can play an important role in many tasks related to ADS perception, including object detection based on both camera and LiDAR data points. Apollo [21] and Autoware [22] are examples of Level-4 ADSs that utilise DNNs to process this data.

It is well-known, however, that DNNs may be susceptible to adversarial attacks in which inputs are manipulated to trigger a misperception. For example, an adversarial object placed in the road’s centre may be ignored by DNN-based camera and LiDAR object detection algorithms [11]; the strategic placement of adversarial patches on a roadside billboard may have a notable impact on the driving behaviour of DNN-based algorithms used by the ADS [23], [24], [25]; a dirty patch on the road surface can cause DNN-based Automated Lane Centering to deviate from the intended steering angle [14]; and the presence of an adversarial patch on the vehicle in front can result in a malfunction of the DNN-based depth estimation algorithm within ADS [15]. Note that these adversarial attacks primarily fall under the category of white-box attacks (i.e. involving patches/objects with suspicious shapes).

However, ensuring the resilience of DNNs against these attacks is a difficult problem. While a few methods [26], [27],

[28], [29] have demonstrated effectiveness against specific categories of adversarial attacks, none of them can serve as a universal solution for countering all types of attacks as highlighted in surveys on adversarial attacks and defences strategies [30], [31], meaning that it remains important to systematically test ADSs against them.

2.2 Attack Goal and Threat Model

Attack Goal. We propose a black box adversarial attack on the perception systems of ADSs, with the goal of inducing behaviour in which the AV violates traffic laws. This must be achieved by objects that follow conventional road design guidelines and appear benign to humans (i.e. no patches or unusual shapes). Such scenarios are termed ‘natural’: they are subsets of all possible scenarios and are characterised by restrictions on the placement of objects like bins, billboards, and greenery. We formulate the attack goal as follows:

Definition 1 (Attack Goal). *Let ϕ denote a user-specific specification of ADS behaviour, and φ denote a formula specifying the rules of natural scenarios. Then, our attack goal is to find a scenario λ such that $\lambda \models \varphi$ and there exists a trace π of the ADS within λ such that $\pi \not\models \phi$.*

In this paper, the attack is divided into two tasks: (1) generate a scenario λ in which the placement of roadside objects satisfies some formalised regulatory rules φ ; and (2) optimise the placement of objects to induce a misperception that causes the ADS to violate a traffic law specification ϕ .

Threat Model. Our attack assumes a black box setting, in which the attacker has no access to the internal details of the perception system and its models. The attacker is only able to observe the outputs of the perception system and chassis information of the ADS. Furthermore, the attacker does not possess any knowledge of the inner architecture of the ADS or any algorithms that it utilises. This ensures that the attack can be used to test the resilience of any ADS by treating its perception system as a black box. The attacker’s ability is limited to modifying and moving roadside objects. They are further *restricted to ‘natural’ object placements* that satisfy government regulations [32] and company guidelines [8], [9], [10] ensuring scenarios are realistic. Furthermore, the attacker cannot utilise adversarial patches, as these appear as visually unnatural and require whitebox knowledge of the perception models, which in our case the attacker does not have.

2.3 Specifying Safety Properties

Our attack goal is to cause misperceptions that result in the violation of safety properties. In the context of AVs, safety should not simply mean the absence of collisions, but also adherence to the rules of the road that drivers are supposed to abide by. To that end, we adopt the property specification language used by LawBreaker [17], as well as the project’s existing specifications of the traffic laws of China and Singapore. The specification language is based on Signal Temporal Logic (STL), and is evaluated with respect to traces of scenes, providing a way to automatically determine whether a tester-defined property was violated or not in a simulated run of the ADS. We highlight the key

$$\begin{aligned}\phi &:= \mu \mid \neg\phi \mid \phi_1 \vee \phi_2 \mid \phi_1 \wedge \phi_2 \mid \phi_1 \mathbf{U}_I \phi_2 \\ \mu &:= f(x_0, x_1, \dots, x_k) \sim 0 \quad \sim := > \mid \geq \mid < \mid \leq \mid \neq \mid =;\end{aligned}$$

Fig. 2: Specification language syntax, where ϕ , ϕ_1 and ϕ_2 are STL formulas, I is an interval, and f is a multivariate linear continuous function over language variables x_i

features of the specification language below (the full syntax and semantics is given in [17]).

The high-level syntax of the language is shown in Figure 2. A time interval I is of the form $[l, u]$, where l and u are respectively the lower and upper bounds of the interval. Following convention, we write $\Diamond_I \phi$ to denote $\text{true} \mathbf{U}_I \phi$; and $\Box_I \phi$ to denote $\neg \Diamond_I \neg\phi$. Intuitively, \mathbf{U} , \Box , and \Diamond are modal operators that are respectively interpreted as ‘until’, ‘always’, and ‘eventually’. We omit the time interval when it is $[0, \infty]$.

In general, μ can be regarded as a proposition of the form $f(x_0, x_1, \dots, x_k) \sim 0$, where f is a multivariate function and x_i for all i in $[0, k]$ is a variable supported in the language.

Example 2.1. *Suppose we have a signal variable $\text{speed} = \langle \text{speed}(0), \text{speed}(1), \dots, \text{speed}(n) \rangle$, which represents the autonomous vehicle’s speed throughout its journey. Then, we can create a simple Boolean Expression $\mu = \text{speed}(t) < 100$ to check whether the speed of the vehicle is larger than 100km/h, as illustrated in Fig 2. Note that μ can be regarded as a proposition of the form $100 - \text{speed}(t) > 0$ or $\text{speed}(t) - 100 < 0$. To verify whether μ holds true at all time steps, we can straightforwardly incorporate the temporal logic symbol “always”, resulting in the formulation of $\varphi = \Box(\text{speed} < 100)$.*

A specification is evaluated with respect to a trace π of scenes, denoted as $\pi = \langle \pi_0, \pi_1, \pi_2, \dots, \pi_n \rangle$, where each scene π_i is a valuation of the propositions at time step i and π_0 reflects the state at the start of a simulation. The language follows the standard semantics of STL (see e.g. [33]).

2.4 Design Challenges

The goals above imply two key design challenges:

C1. Restricting to ‘natural’ scenarios. A key objective of our work is to develop attack scenarios that appear as completely ‘natural’ to humans. Previous work, such as NADE [34], has focused on replicating natural driving behaviours of vehicles. In contrast, our focus is on the strategic placement of typical roadside objects, including (but not limited to) trash bins, trees, and fire hydrants. A significant challenge is knowing when the placement of such objects crosses the boundary between something innocuous to something suspicious. To that end, we constrain the placement of objects according to existing regulations and guidelines (e.g. [32], [8], [9], [10]), which we use to standardise the notion of natural scenarios.

In addition, by restricting our scenarios to natural ones, we impose constraints that significantly reduce the available space of modifications, requiring testing algorithms that navigate them more creatively. We cannot arbitrarily modify the environment that the ADS is driving in. For example, placing a trash in directly in the middle of the road should

be forbidden in our testing context, as this is clearly an unnatural scenario that violates standard guidelines on bin placement.

C2. Large black-box search space. Despite restricting the placement of objects to conventional road design guidelines, there remains an enormous number of possible combinations of placements, making the search space vast and challenging to navigate, particularly in a black box setting. For example, even when limiting to only 10 permissible placement locations, if each of them can be occupied by one of 10 different possible objects, we already have 10^{10} combinations of object placements. Hence, an effective search algorithm is necessary.

3 ATTACK DESIGN

We propose TrashFuzz to address the challenges highlighted in Section 2.4 as described in the following.

3.1 Generating Natural Scenarios (C1)

As mentioned, we overcome C1 by utilising existing regulations and guidelines for the placement of various roadside objects. In particular, we refer to government documents including the Code of Practice for Works on Public Streets (COP) [5] and Guidelines on Greenery Provision and Tree Conservation (GGPTC) [7]. The COP, formulated by Singapore’s Land Transport Authority, delineates the necessary procedures and regulations for conducting activities on public roads, whereas the GGPTC, introduced by Singapore’s National Parks Board, governs the placement and preservation of trees within urban landscapes. For the placement of trash bins, we refer to the guidelines provided by three prominent recycling companies: HDS, KIMBLE, and GRANGER [8], [9], [10].

We formalise the notion of natural scenario by translating the regulations/guidelines described in these documents into mathematical formulas. Though in natural language, the guidelines are quite specific, allowing for a relatively direct translation of the rules to formulas. Table 1 lists these 12 specifications along with some descriptions. Specifications 1–3 refer to section 6.5 of the COP [5]. Specifications 4–8 refer to pages 95–97 of the GGPTC [7]. Specifications 9–11 pertain to key aspects of the guidelines provided by the waste recycling companies [8], [9], [10]. Note that while we have focused on guidelines from one country to ensure consistency between our rules, the general approach of formalising rules can be applied to the guidelines of any other country or jurisdiction.

In our rules, the function $dis(a, b)$ returns the distance between two objects, a and b , while the function $lanenum(road)$ returns the count of lanes within the designated *road*. Each distinct category of objects is denoted by a class variable. For example, the class *tree* serves as a general representation for trees and includes a characteristic attribute, *tree.h*, corresponding to height.

It is crucial to have a diverse range of attack objects at our disposal. Several simulators, including AWSIM [35] and LGSVL [19]), are built upon the Unity Real-Time Development Platform [36]. The Unity Asset Store [20] has a vast library of 3D asset packages, with an open-door policy

that allows anyone to contribute their creations. Each asset package provides necessary elements, such as meshes of 3D objects and 2D textures, for constructing objects inside the simulators. We can access thousands of objects that are commonly encountered during driving such as rocks, trash bins, and hydrants for free. Hence, our strategy involves exploring Unity’s asset library [20] to discover suitable adversarial objects.

In this work, we leverage a variety of freely accessible 3D asset packages from the Unity Asset Store [20] to integrate commonly encountered roadside objects. These include trash bins in a variety of shapes and colours, benches constructed from different materials and exhibiting various shapes, a wide array of tree types, hydrants, and trash bags. Crucially, these objects can be effortlessly spawned within Unity-based simulators, such as LGSVL [19]. We provide all these assets on our website [37], offering a convenient way for users to integrate them into the LGSVL simulator environment directly.

3.2 Greedy Gradient-Guided Black Box Search (C2)

We require an efficient algorithm for identifying suitable attack scenarios in a black box setting. Given our objective is to induce ADS behaviours that violate traffic law specifications, it is important that the algorithm can uncover *different* ways to violate the specification. For instance, consider the specification $speed > 10 \wedge speed < 100$. There are two distinct ways to violate it: first by inducing *speed* to a value smaller than 10, and second by inducing it to a value larger than 100.

In this section, we present the detailed design of our algorithm. Given the time-consuming nature of simulator-based evaluations for ADSs, our primary goal is to attain convergence as fast as possible. To achieve this, our algorithm is ‘greedy’, in the sense of initially exploring adversarial scenarios that appear most likely to violate the given specification, and is also ‘gradient guided’, in the sense that it systematically expands its exploration based on these initial findings.

We present the algorithm in three parts. First, we delve into the encoding of (natural) scenarios as vectors, which forms the foundation of subsequent steps (e.g. mutation). Second, we present the design of our objective function which provides a quantified way to sufficiently ‘cover’ different ways of violating a specification, ensuring diversity in the results. Finally, we introduce our new greedy gradient-guided search algorithm, which forms the core of the approach.

3.2.1 Encoding of Scenarios

We represent each adversarial scenario as a vector ϕ with dimensions $n \times d$. Here, n refers to the number of adversarial objects, while d corresponds to the four essential dimensions of each adversarial object: *forward*, *right*, *rotation*, and *type*. The *forward* and *right* dimensions indicate the relative position of the adversarial object with respect to the start position of the ego vehicle. For example, if the value for *forward* is 10, and the value for *right* is -2 , the object is located at the left front of the ego vehicle. The *rotation* dimension represents the placement angle of the adversarial

TABLE 1: Specifications for ‘natural’ scenarios, based on public road design guidelines

rule1	The fixed position attack objects should not be on the road or footway. $dis(obj.fix, road) \neq 0 \wedge dis(obj, footway) \neq 0$
rule2	The fixed position attack objects (OG Boxes) should be at least 0.6 meters away from the main road. The main road refers to a road with at least two lines. $lanenum(road) \geq 2 \implies dis(obj.fix, road) > 0.6$
rule3	The fixed position attack objects (OG Boxes) cannot be put near the minor road. A minor road refers to a road with one line. $lanenum(road) < 2 \implies dis(obj.fix, road) > 10$
rule4	The splay corner of the entrance culvert, bin centre access, substation access, MDF room access, and fire engine access should be at least 1m to Palm, 1.5m from a small to medium tree, and 2.5m from a large tree. $(tree.h < 1.5 \implies dis(tree, corners) > 1) \wedge (tree.h \geq 1.5 \wedge tree.h < 5 \implies dis(tree, corners) > 1.5) \wedge (tree.h \geq 5 \implies dis(tree, corners) > 2.5)$
rule5	The scupper pipe/drain should be at least 1m from a Palm, 1.5m from a small to medium tree and 2.5m from a large tree. $tree.h < 1.5 \implies dis(tree, pipe) > 1 \wedge (tree.h \geq 1.5 \wedge tree.h < 5) \implies dis(tree, pipe) > 1.5 \wedge tree.h \geq 5 \implies dis(tree, pipe) > 2.5$
rule6	The trees should be at least 3m from a Lamp post. $dis(tree, lamp) > 3$
rule7	The fixed position attack objects (OG Boxes), TAS manhole, sewer line, manhole, electrical post, fire hydrant, SCV box, lighting control box, traffic control box, traffic lights, or lightning pits should be at least 2m to Palm or small to medium trees, and 2.5m to large trees. $tree.h < 5 \implies dis(tree, obj.fix) > 2 \wedge tree.h \geq 5 \implies dis(tree, obj.fix) > 2.5$
rule8	Trees should be at least 3m from the edge of a footpath crossing. $dis(tree, footpath) > 3$
rule9	Trash bins should not block the road or footpath. $dis(bin, road) > 0 \wedge (dis(bin, footpath) > 0 \vee footpath.width - bin.width > 1.5)$
rule10	Trash bins should maintain a minimum distance of 0.5 meters from each other and other objects like mailboxes, walls, lamp posts, utility boxes, vehicles, etc. $dis(bin, obj) \geq 0.5$
rule11	Wheels and handles of trash bins should be placed away from the road. $bin.direction \times road.direction < 0.2$
rule12	Make sure nothing is in between the trash bins and the road. $dis(obj, road) + dis(bin, obj) > dis(bin, road)$

TABLE 2: An example of an encoded scenario

Adversarial Objects	forward	right	rotation	type
obstacle1	25.04	2.63	25.78°	Bench1
obstacle2	49.45	6.23	9.21°	BigTrashBin
obstacle3	60.55	4.14	91.98°	TrashBin(Yellow)
obstacle4	57.85	7.98	49.89°	TrashBin(Red)
obstacle5	18.95	-9.83	290.48°	TrashBin(Green)

object. The *type* is a sequence number corresponding to the adversarial objects library, allowing us to easily identify and categorise different types of adversarial objects. In addition, each scenario also provides the initial and destination positions for the ADS journey.

Table 2 provides an example scenario encoding. Within this scenario, there are five adversarial objects. Four of these objects, namely a bench, a large trash bin, a yellow trash bin, and a red trash bin, are strategically placed to the front-right of the ego vehicle’s starting point, each with distinct rotation angles (designated as *obstacle1*...4). Additionally, a green trash bin is positioned in the front-left with a rotation angle of 290.48 degrees, labelled as *obstacle5*.

3.2.2 Coverage-based Objective Function Design

We treat the attack generation process as an optimisation problem.

Definition 2. Let Θ be a set of property specifications and Λ a set of adversarial scenarios. Our optimisation problem is:

$$\text{Minimise : } \sum_{\phi \in \Theta} \min_{\lambda \in \Lambda} \{\rho(\phi, \pi_\lambda)\}$$

where π_λ is the trace of ADS in the face of an adversarial scenario λ and function $\rho(\phi, \pi)$ is the robustness value of trace π evaluated under specification ϕ .

We thus require a set of adversarial scenarios that minimises the robustness function across several property specifications. Intuitively, the robustness function reflects

the *distance* to a specification violation, meaning it measures how close the current trace π is to violating the specification. Firstly, we must establish a precise definition for the fundamental *objective function*, denoted as $\rho(\phi, \pi)$. Secondly, we require a systematic approach to replace the specification with a set of smaller formulas (Θ), each one characterising a different way to violate the original specification. Note that we adapt the quantitative semantics and decomposition from LawBreaker [17].

Quantitative Semantics. We define our objective function using the quantitative semantics of STL [33], [38], [39], which produces a numerical *robustness* degree.

Definition 3 (Quantitative semantics). Given a trace π and a formula ϕ , the quantitative semantics is defined as the robustness degree $\rho(\phi, \pi, t)$, computed as follows. Recall that propositions μ are of the form $f(x_0, x_1, \dots, x_k) \sim 0$.

$$\rho(\mu, \pi, t) = \begin{cases} -\pi_t(f(x_0, x_1, \dots, x_k)) & \text{if } \sim \text{ is } \leq \text{ or } < \\ \pi_t(f(x_0, x_1, \dots, x_k)) & \text{if } \sim \text{ is } \geq \text{ or } > \\ |\pi_t(f(x_0, x_1, \dots, x_k))| & \text{if } \sim \text{ is } \neq \\ -|\pi_t(f(x_0, x_1, \dots, x_k))| & \text{if } \sim \text{ is } = \end{cases}$$

where t is the time step and $\pi_t(e)$ is the valuation of expression e at time t in π .

$$\begin{aligned} \rho(\neg\phi, \pi, t) &= -\rho(\phi, \pi, t) \\ \rho(\phi_1 \wedge \phi_2, \pi, t) &= \min\{\rho(\phi_1, \pi, t), \rho(\phi_2, \pi, t)\} \\ \rho(\phi_1 \vee \phi_2, \pi, t) &= \max\{\rho(\phi_1, \pi, t), \rho(\phi_2, \pi, t)\} \\ \rho(\phi_1 \text{ U}_I \phi_2, \pi, t) &= \sup_{t_1 \in t+I} \min\{\rho(\phi_2, \pi, t_1), \inf_{t_2 \in [t, t_1]} \rho(\phi_1, \pi, t_2)\} \end{aligned}$$

where $t + I$ is the interval $[t + t, u + t]$ given $I = [l, u]$. \square

Intuitively, this quantitative semantics computes how ‘close’ the ADS is from violating the given property specification ϕ . Note that the smaller $\rho(\phi, \pi, t)$ is, the closer π is to violating ϕ . If $\rho(\phi, \pi, t) \leq 0$, this means ϕ is violated. We write $\rho(\phi, \pi)$ to denote $\rho(\phi, \pi, 0)$; $\pi \models \phi$ to denote

$\rho(\phi, \pi, t) > 0$; and $\pi \not\models \phi$ to denote $\rho(\phi, \pi, t) \leq 0$. Note that time is discrete in our setting.

Example 3.1. Let $\varphi = \Box(\text{speed} < 100)$, i.e. the speed limit is 100km/h. Suppose $\pi = \langle (\text{speed} \mapsto 0, \dots), (\text{speed} \mapsto 0.5, \dots), \dots (\text{speed} \mapsto 90, \dots) \rangle$, where the ego vehicle's max speed is 90km/h at the last time step. We have $\rho(\varphi, \pi) = \rho(\varphi, \pi, 0) = \min_{t \in [0, |\pi|]} (100 - \pi_t(\text{speed})) = 10$. This means that trace π satisfies φ , and the robustness value is 10.

Deriving 'Violation Goals' from a Specification. We transform a specification into a set of smaller formulas, such that the violation of any one formula implies the violation of the original specification. The rationale is that this will allow us to evaluate the robustness degree with respect to multiple different ways of violating the original specification, rather than just focusing on the 'easiest' one. Here, we adopt the methodology of LawBreaker [17], which defines a method to derive a set of violation goals based on the given complex specification ϕ . We write $\Theta(\phi)$ to denote a set of 'violation goals' of ϕ , i.e. that satisfy the following proposition:

Proposition 3.2. For STL formulas ϕ and traces π :

$$\forall \varphi \in \Theta(\phi). \pi \not\models \varphi \implies \pi \not\models \phi$$

The set of violation goals $\Theta(\phi)$ is calculated as follows:

$$\begin{aligned} \Theta(\mu) &= \{\mu\}; \Theta(\neg\phi) = \Theta(N(\phi)); \\ \Theta(\phi_1 \wedge \phi_2) &= \Theta(\phi_1) \cup \Theta(\phi_2); \Theta(\bigcirc\phi) = \{\bigcirc x \mid x \in \Theta(\phi)\}; \\ \Theta(\phi_1 \mathcal{U}_I \phi_2) &= \{x \mathcal{U}_I y \mid x \in \Theta(\phi_1) \wedge y \in \Theta(\phi_2)\}; \end{aligned}$$

Here, μ is a Boolean expression and function $N(\phi)$ returns the negation of the formula ϕ without operator \neg . This eliminates the need for an additional calculation to determine $\Theta(\neg\phi)$, as all formulas containing the operator \neg have already been transformed into their equivalent formulas without operator \neg .

Proposition 3.3. For STL formulas ϕ and traces π :

$$\forall \phi. \forall \pi. \rho(N(\phi), \pi) = \rho(\neg\phi, \pi).$$

Definition 4 (Specification Negation). Given a specification formula ϕ , the negation of this formula, $N(\phi)$, is defined:

$$\begin{aligned} N(\mu) &= n(\mu); N(\neg\phi) = \phi; N(\phi_1 \wedge \phi_2) = N(\phi_1) \vee N(\phi_2); \\ N(\phi_1 \vee \phi_2) &= N(\phi_1) \wedge N(\phi_2); N(\bigcirc\phi) = \bigcirc N(\phi); \\ N(\phi_1 \mathcal{U}_I \phi_2) &= (\Box_I N(\phi_2)) \vee (N(\phi_2) \mathcal{U}_I (N(\phi_1) \wedge N(\phi_2))); \end{aligned}$$

where $n(\mu)$ is defined as follows:

$$n(\mu) = \begin{cases} e_1 \geq (\text{resp. } >) e_2 & \text{if } \mu \text{ is } e_1 < (\text{resp. } \leq) e_2; \\ e_1 \leq (\text{resp. } <) e_2 & \text{if } \mu \text{ is } e_1 > (\text{resp. } \geq) e_2 \\ e_1 \neq (\text{resp. } =) e_2 & \text{if } \mu \text{ is } e_1 = (\text{resp. } \neq) e_2 \end{cases}$$

Propositions 3.2 and 4 can be proved by structural induction. We refer the readers to [17], [40] for the detailed proofs.

Example 3.4. The value of $\Theta(\phi)$ is calculated recursively. For example, given a specification $\phi = \Box(\mu_1 \wedge \mu_2)$, we can get $\Theta(\phi)$ as follows:

- 1) First step is to deal with calculations of primitive elements:
 $\Theta(\mu_1) = \{\mu_1\}, \Theta(\mu_2) = \{\mu_2\}$
- 2) Then we have: $\Theta(\mu_1 \wedge \mu_2) = \Theta(\mu_1) \cup \Theta(\mu_2) = \{\mu_1, \mu_2\}$

3) Given $\Theta(\mu_1 \wedge \mu_2)$, we can get:

$$\Theta(\Box(\mu_1 \wedge \mu_2)) = \{\Box(\mu_1), \Box(\mu_2)\}$$

4) The final result is $\Theta(\phi) = \{\Box(\mu_1), \Box(\mu_2)\}$.

i.e. there exist two violation goals for ϕ , and the violation of either one of them can result in the violation of ϕ .

3.2.3 Greedy Gradient Guided Query

With the derivation of violation goals reviewed, we now propose our new greedy gradient-guided query algorithm. We first describe the gradient calculation process before presenting the algorithm as a whole.

Gradient Calculation. In our black-box setting, gradient calculations are important for guiding the generation of adversarial scenarios. These gradients are constructed by differentiating between the original scenario and the scenario following the modifications. We define the gradient calculation below:

Definition 5. Let ϕ be a property specification, λ be the initial scenario, λ' be the scenario after modification, and $E(\lambda)/E(\lambda')$ denote the encoding of scenario λ/λ' . The gradient calculation is formally defined as follows:

$$G(\lambda, \lambda', \phi) = \frac{\rho(\phi, \pi) - \rho(\phi, \pi')}{E(\lambda) - E(\lambda')}$$

where π and π' correspond to the traces of the ADS in response to scenarios λ and λ' , respectively.

Intuitively, the gradient calculation reveals the extent to which modifying the scenario influences the behaviour of the ADS. A positive gradient value signifies that the current modification enhances robustness with respect to the property specification, while a negative gradient value suggests a decrease in robustness due to the modification. Furthermore, the magnitude of the gradient value reflects the magnitude of the modification's impact on the robustness value.

Overall Algorithm. The overall algorithm is shown in Algorithm 1. First, we prepare a random scenario as our initial test case and calculate the subdivisions of the user-given specification φ to obtain Θ_r , then initialize *seed* with *seed.gradient* value 0 and *seed.element* value *Null*. Note that *seed* is a pair storing gradient value and a corresponding scenario.

Next, using the initial adversarial scenario λ_0 , we execute it to generate the trace π_0 . The adversarial scenario contains several adversarial objects, and for each of these objects, we apply random mutations to create new scenarios. Note that the mutations have been designed to ensure that the ADS remains compliant with the rules listed in Table 1, as well as with other physical constraints such as the requirement for objects to be grounded. For each newly generated scenario, we also execute it to produce a trace and assess it against all the remaining specifications in set Θ_r . We remove φ from the set if it is violated, i.e. if $\rho(\xi, \pi_i) \leq 0$, and add the corresponding scenario λ_i to the output set Γ . After executing and processing all the cases generated by the initial test case, we utilise the gradient calculation defined above to choose the seed for the next round. In essence, we designate the case with the largest absolute gradient value as the seed for the subsequent round.

Algorithm 1: The TrashFuzz Algorithm

Input: ϕ , n (number of adversarial objects), and M (maximal queries)
Output: A test suite Γ

- 1 Let $\Theta_r = \Theta(\phi)$ be the set of uncovered formulas in $\Theta(\phi)$;
- 2 Let $seed$ be a pair of a gradient value and a mutable element; initially the gradient value $seed.gradient$ is 0 and the mutable element $seed.element$ is $Null$;
- 3 Let λ_0 be a randomly generated adversarial scenario;
- 4 Let Γ be an empty set;
- 5 **while** Θ_r is not empty and not timeout **do**
 - 6 Execute λ_0 via simulation and obtain trace π_0 ;
 - 7 Mutate each adversarial object in λ_0 and get a few adversarial scenarios $\lambda_1, \dots, \lambda_n$;
 - 8 Execute $\lambda_1, \dots, \lambda_n$ via simulation and obtain trace π_1, \dots, π_n ;
 - 9 **for each** π_k in π_1, \dots, π_n **do**
 - 10 **for each** φ in Θ_r **do**
 - 11 **if** $\rho(\varphi, \pi_k) \leq 0$ **then**
 - 12 Remove φ from Θ_r ; Add s_k into Γ ;
 - 13 **end**
 - 14 **else if** $|G(\lambda_0, \lambda_k, \varphi)| > |seed.gradient|$ **then**
 - 15 $seed.gradient = G(\pi_0, \pi_k, \varphi)$;
 - 16 Store the mutated element of s_k to $seed.element$;
 - 17 **end**
 - 18 **end**
 - 19 **end**
 - 20 Generate the next s_0 based on $seed$;
 - 21 **end**
 - 22 **return** Γ

This process is repeated until all the elements in set $\Theta(\phi)$ are covered or the maximal number of generations M (as defined by the user) has been reached.

4 IMPLEMENTATION AND EVALUATION

In this section, we present our implementation of TrashFuzz for the Apollo ADS and evaluate its effectiveness in identifying natural scenarios that lead to traffic law violations, as well as other key aspects. For additional experimental materials and results, we direct readers to our website [37].

4.1 Implementation

Implementing TrashFuzz involves three broad steps. First, some basic integration with and between the existing ADS and simulator, including a communication bridge, a trace generator, and the means of both checking a specification as well as calculating its robustness with respect to a trace. Second, the generation of natural scenarios consisting of (benign-appearing) adversarial roadside objects, as detailed in Section 3.1. Finally, the implementation of our greedy gradient-based fuzzing engine, as elaborated on in Section 3.2.

The target of our evaluation is version 7.0 of the Apollo ADS [18] (the most recent version at the time of experimentation) with the LGSVL [19] simulator. To establish communication between Apollo and LGSVL, we utilise the official communication bridge, CyberRT [41]. For trace generation and specification evaluation/robustness, we use the implementation strategy described by LawBreaker [17]. In particular, the trace generator creates a trace π by processing

TABLE 3: Percentage of valid scenarios

Atk Obj	1	2	3	4	5	6	7
Rand	rule1	79.9	63.7	50.1	39.9	32.5	25.2
	rule2-3	77.7	60.2	46.2	35.2	28.3	21.1
	rule4-6	91.1	83.5	76.3	69.0	63.6	57.4
	rule9	85.1	73.7	62.9	53.9	45.8	38.3
	rule10	100	99.99	99.98	99.99	99.97	99.96
	rule11	89.2	80.7	71.5	64.9	58.0	51.8
	rule12	100	100	100	100	100	100
	all	56.0	32.0	17.6	10.1	5.8	3.1
Ours	all	100	100	100	100	100	100

messages subscribed to by the ADS, whereas for specifying traffic laws, we utilise the domain-specific language provided by LawBreaker. To implement the quantitative semantics of those traffic laws, we embedded the *RTAMT* tool [39] to compute the robustness of the specifications with respect to the trace obtained from the bridge. (Note that implementing TrashFuzz for Autoware/CARLA follows a largely similar strategy, except for substituting the ROS bridge [42] for CyberRT.)

In order to generate natural scenarios, we sourced common roadside objects from the Unity Asset Store [20]. As LGSVL is a Unity-based simulator, these could be directly placed into scenarios. The roadside objects we utilised in TrashFuzz have been assembled into a single library that we have made available online [37]. To ensure the objects are placed according to conventional road design guidelines, we constrained their placement according to the functions in Table 1. These functions take a scenario as input and return a Boolean value to indicate whether the generated scenario is valid or not according to the guidelines.

Finally, we integrated the above components and implemented our greedy gradient-based fuzzing engine as described in Section 3.2. Our experiments were conducted using two machines, each equipped with 32GB of memory, an Intel i7-10700k CPU, and an RTX 2080Ti graphics card. These two machines run on Linux (Ubuntu 20.04.5 LTS) and Windows (Windows 10 Pro) operating systems, respectively.

4.2 Evaluation

We conducted experiments to answer four Research Questions (RQs).

- **RQ1:** Can TrashFuzz produce valid scenarios?
- **RQ2:** Can natural attack scenarios cause traffic law violations?
- **RQ3:** Can our greedy gradient-based search algorithm cover more violations than the most comparable fuzzer?
- **RQ4:** Can TrashFuzz be used to test different ADSs?
- **RQ5:** How difficult is it to carry out TrashFuzz attacks?

RQ1: Can TrashFuzz produce valid scenarios? Given the specifications shown in Table 1, we first investigate whether TrashFuzz can effectively generate valid scenarios that satisfy them. We compare TrashFuzz with randomly generated scenarios. Our evaluation involved analyzing 10,000 randomly generated scenarios, each with a fixed number of attack objects. Note that in these scenarios, we randomly place attack objects within a designated area, i.e., a 150m \times 60m space in front of the AV. The results are shown in Table 3. Here, the numbers (1 to 7) in the first row indicate the number of attack objects. We present the

TABLE 4: Violations of traffic laws while TrashFuzz operates under imposed restrictions

Traffic Laws	LawBreaker	TrashFuzz	Law Concerns
Law38	sub1	✓	green light
	sub2	✓	yellow light
	sub3	✓	red light
Law44	✓	✓	lane change
Law45	sub1	×	speed limit
	sub2	×	speed limit
Law46	sub2	✓	speed limit
	sub3	✓	speed limit
Law47	✓	✓	overtake
Law50	×	×	reverse
Law51	sub3	✓	traffic light
	sub4	✓	traffic light
	sub5	✓	traffic light
	sub6	×	traffic light
	sub7	×	traffic light
Law52 sub2-4	×	×	priority
Law53	×	×	traffic jam
Law57	sub1	✓	left turn signal
	sub2	✓	right turn signal
Law58	✓	✓	warning signal
Law59	✓	✓	signals
Law62 sub8	×	×	honk

TABLE 5: Number of traffic law violation goals (out of a possible 82) covered for the Apollo ADS

Num	Driver	Alg.	R1	R2	R3	R4	Avg
7	Apollo	LawBreaker	23	15	19	16	18.25
		TrashFuzz	17	22	19	21	19.75
6	Apollo	LawBreaker	15	15	13	22	16.25
		TrashFuzz	19	16	18	21	18.5
5	Apollo	LawBreaker	13	16	14	13	14
		TrashFuzz	21	16	15	20	18
4	Apollo	LawBreaker	17	16	13	14	15
		TrashFuzz	17	15	16	14	15.5
3	Apollo	LawBreaker	14	9	14	11	12
		TrashFuzz	17	16	16	14	15.75
2	Apollo	LawBreaker	11	14	11	10	11.5
		TrashFuzz	14	15	10	13	13
1	Apollo	LawBreaker	12	14	10	9	11.25
		TrashFuzz	13	11	17	12	13.25
0	Apollo	-	7	9	5	7	7

percentage of scenarios that satisfy the given specification. A higher percentage value indicates a greater number of valid scenarios. Rule2 and rule3 have been merged into one specification concerning the distance of fixed-position objects from the road. Likewise, rule4–6 are combined into one specification that evaluates the positioning of trees. This analysis demonstrates that a majority of the randomly generated scenarios are invalid with respect to public road design guidelines. Moreover, as the number of attack objects increases, the likelihood of scenarios deviating from these guidelines rises. This result indicates that most randomly generated scenarios are not ‘natural’. For instance, these objects are often placed directly on the road, a violation of rule1 or rule9 as outlined in Table 1. As shown by the final row of Table 3, TrashFuzz succeeds in generating a higher proportion of natural scenarios with respect to the placement guidelines in Table 1.

RQ2: Can natural attack scenarios cause traffic law violations? To answer this question, we applied our fuzzing algorithm to systematically test all testable traffic law specifications (including the multiple sub-laws) provided with the LawBreaker [17] tool. Our experiment covered all ‘testable’ laws, excluding those that cannot be tested due to limitations in the simulator. For instance, traffic regulations related to traffic lights with arrow lights are non-testable

because LGSVL only supports traffic lights with circular lights.

The results are summarised in Table 4. Here, we present all the testable laws applicable to AVs within the platform. However, certain other relevant laws cannot be tested due to limitations in the available maps. For example, law 49 regulates that vehicles should not make U-turns at railway crossings, sharp bends, steep slopes, or tunnels. Unfortunately, the current maps of existing platforms (LGSVL and CARLA) do not include representations of these specific locations, rendering them untestable under the current conditions.

Within this table, the ‘LawBreaker’ and ‘TrashFuzz’ columns indicate whether Apollo violated the specific traffic regulation listed in the first two columns. We mark ✓ for a traffic law ϕ if and only if $\pi \not\models \phi$ happened for a scenario generated by LawBreaker or TrashFuzz. We conducted multiple test runs, repeating the corresponding test cases at least three times to confirm and ensure the reproducibility of all issues. Note that the tools are violating laws using different mutation strategies: LawBreaker mutates the driving behaviour of other vehicles and pedestrians, whereas TrashFuzz instead mutates the placement of roadside objects subject to the roadside design guidelines (Table 1). TrashFuzz’s strategy is much more challenging due to the additional restrictions entailed.

As can be seen from the table, even while constrained to satisfy road design guidelines, TrashFuzz still manages to incite violations of a majority of the traffic laws. In comparison to LawBreaker, TrashFuzz covers all the traffic laws that LawBreaker violates. Additionally, TrashFuzz has the capability to activate an additional sub-law, specifically sub-law 7 of Article 51, which regulates that turning vehicles yield to straight-moving vehicles, whereas pedestrians and right-turning vehicles travelling in the opposite direction yield to left-turning vehicles. The activation of this supplementary sub-law is triggered by the presence of adversarial objects along the roadside. Note that TrashFuzz found an additional law violation compared to LawBreaker *despite the restriction* to modifying roadside object placements only.

We identified two broad categories of issues among the tests generated by TrashFuzz, which we elaborate on below. These misjudgments stem from flaws in the perception system of the ADS. While the camera images and lidar points received by the ADS from the simulator appear normal, the system arrives at incorrect judgments. Note that we repeat the following issues at least three times to ensure their reproducibility.

Classification and Segmentation Errors. The first category of issues concerns misclassification of adversarial objects or malfunctions in the segmentation algorithm. For example, in some adversarial situations, trash bins may be erroneously classified as pedestrians or bicycles. In such cases, the ADS fails to identify these trash bins as stationary obstacles, which could potentially lead to collisions or other safety concerns (e.g. waiting for a ‘pedestrian’ to move when it is really a trash bin). Moreover, the deliberate placement of two trash bins in close proximity is intended to deceive the AV’s perception system into perceiving them as a single object such as a vehicle. This misclassification has the potential to confuse the vehicle’s decision-making algorithms, potentially causing hesitation or preventing the vehicle from

taking appropriate action, particularly at intersections. Furthermore, when a trash bin is positioned lying down and adjacent to a bench, there are instances where the ADS fails to segment them separately, recognising them as a single unknown object. Note that these misclassifications are not limited to a single frame; rather, they last for a significant duration, propagating throughout the entire system and potentially inducing subsequent misbehavior, e.g. the ADS hesitating and failing to proceed as intended.

Overloaded Perception System. The second category of issues concerns the perception system of the ADS, which in general, is complex and consists of multiple algorithm and modules. In issues of this category, a few adversarial objects are strategically placed at specific positions along the ADS’s route to deny the service of the traffic light perception system of the ADS. In this situation, the traffic light perception system becomes overloaded, resulting in anomalous outputs. We observed two possible consequences of this situation in our tests. In the first, the roadside objects deceive the AV into perceiving the traffic light ahead as a red or yellow traffic light. This would cause the vehicle to interpret the intersection as a signal to stop indefinitely, regardless of the absence of an actual red traffic light or any other vehicles or pedestrians. Such a misperception can disrupt the normal flow of traffic and potentially lead to congestion or delays. In the second, we deceive the autonomous vehicle into perceiving the traffic light ahead as a green traffic light. Consequently, the detection system always indicates a green signal for the traffic light ahead, regardless of its actual state. This situation can lead to dangerous driving behaviours, such as rushing red lights, endangering the AV itself and others on the road.

RQ3: Can our greedy gradient-based search algorithm cover more violations than the most comparable fuzzer? To answer this question, we do a baseline comparison of TrashFuzz’s gradient-based search algorithm against the coverage-based fuzzing algorithm of LawBreaker [17], which is based on a genetic algorithm (GA) [43]. In particular, after decomposing traffic law specifications into violation goals (Section 3.2.2), we compare the coverage of the two tools in the sense of how many of those goals they are able to induce Apollo to satisfy.

LawBreaker’s GA—the baseline in this experiment—begins by creating a generation of test scenarios and subsequently applies mutations and crossovers to produce the next generation. Intuitively, individuals with superior performance effectively ‘survive’ and contribute to the creation of the subsequent generations. In LawBreaker’s fuzzing algorithm, we initialise the population with 30 individuals and run the algorithm for 20 generations, resulting in a total of 620 test cases generated in a single execution. For TrashFuzz, we configure it to allow a maximum of 620 queries, aligning with Lawbreaker’s fuzzing algorithm. Note that LawBreaker concentrates on altering the behavior of NPC vehicles and pedestrians on the road, while the focus of TrashFuzz is instead on modifying the placement of roadside objects. Therefore, to ensure a fair and meaningful comparison, we adopt identical test case encoding methodologies for both LawBreaker and TrashFuzz, as detailed in Section 3.2.1. Additionally, we apply the same scenario restrictions outlined in Table 1 to LawBreaker’s

TABLE 6: Testing Apollo’s perception system

Object	Type	Vehicle?	Bicycle?	Ped?	Ignore?
TrashBin(Grey)	Movable	✓	✓	✓	×
TrashBin(Yellow)	Movable	✓	✓	✓	×
TrashBin(Blue)	Movable	✓	✓	✓	×
TrashBin(Red)	Movable	✓	✓	✓	×
BigTrashBin	Movable	✓	×	×	×
ShoppingCart	Movable	×	×	×	✓
WarningStand	Movable	×	×	×	✓
TrashBag	Movable	×	×	×	✓
Bench0	Fixed-Pos	×	✓	×	✓
Bench1	Fixed-Pos	✓	✓	×	✓
BusStopPole	Fixed-Pos	×	×	×	✓
Hydrant	Fixed-Pos	×	×	×	✓
Tree0	Fixed-Pos	×	×	×	✓
Tree1	Fixed-Pos	×	×	×	✓
Tree2	Fixed-Pos	×	×	×	✓

TABLE 7: Testing Autoware’s perception system

Object	Type	Vehicle?	Bicycle?	Ped?	Ignore?
Chair	Movable	×	✓	✓	✓
Parasol	Movable	×	✓	×	✓
TrashBin	Movable	×	×	✓	×
LandscapeSign	Fixed-Pos	✓	×	×	✓
Mailbox	Fixed-Pos	×	×	✓	✓
Bench	Fixed-Pos	✓	×	×	✓
Pine	Fixed-Pos	×	×	✓	✓
Stall	Fixed-Pos	✓	×	×	✓
Fence	Fixed-Pos	✓	×	×	✓
Hydrant	Fixed-Pos	×	×	✓	✓

fuzzing algorithm, to ensure our comparison solely assesses efficiency of the algorithms under equivalent conditions.

The results are summarised in Table 5. The overall traffic law specification ϕ we use is derived from LawBreaker [17], which contains 24 different Chinese traffic laws that can be decomposed into 82 possible violation goals ($\Theta(\phi)$). In the table, the ‘Num’ column denotes the quantity of adversarial objects involved in the respective attack scenario, ranging from 0 to 7. When the number is 0, it indicates that scenario is a common one without any attack. The ‘R1–4’ columns indicate how many of the 82 possible violation goals for ϕ are covered across four rounds of experimentation, where the average number is given in the last column. As shown, for both LawBreaker and TrashFuzz, the coverage of violations increases proportionally with the number of adversarial objects. Furthermore, TrashFuzz surpasses LawBreaker in covering more violations within a limited number of queries.

RQ4: Can TrashFuzz be used to test different ADSs? The attack carried out by TrashFuzz exploits the vulnerabilities in the perception algorithms of ADSs. These vulnerabilities are not limited to Apollo. We evaluated the perception of Autoware with the Carla simulator [44] as well. Here, we position adversarial objects at random locations along the AV’s path, varying their angles, and evaluate the perception results to determine whether the system ignores or misclassifies them.

In Table 6 and Table 7, we present the results of the evaluations for Apollo (v7) and Autoware (Autoware.ai v1.14), respectively. The ‘Object’ column displays the name of each object, while the ‘Type’ column indicates whether the object is movable or of fixed-position. The ‘Vehicle?’, ‘Bicycle?’, ‘Pedestrian?’, and ‘Ignore?’ columns respectively check whether the perception of the ADS classifies the object as a vehicle, bicycle, pedestrian, or if it is ignored. It is worth noting that both Apollo and Autoware exhibit misclassifications for common objects along the road un-

der certain circumstances. These misclassifications expose potential vulnerabilities in the perception system of these autonomous driving systems.

RQ5: How difficult is it to carry out TrashFuzz attacks?

To answer this question, we propose a comparison between the prerequisites of existing attacks and those of TrashFuzz. The results are shown in Table 8. Within the table, the categories of ‘Patch?’, ‘Shape?’, ‘Placement?’, and ‘Special?’ respectively assess whether the listed attack necessitates a specialised adversarial patch, alters the shape of the adversarial object, designates specific locations for placing adversarial elements, or requires unique equipment unlikely to be found on the roadside (e.g., commercial drones, digital LiDAR spoofers, and projectors). Furthermore, ‘White-B?’, ‘Grey-B?’ and ‘Black-B?’ categorise the type of attack. We mark \checkmark in the table to denote alignment with each criterion. For example, the MSF-Attack [11] alters the shape of objects (e.g. traffic cones) to make them invisible to the camera and LiDAR detection algorithm. Hence, *Shape?* and *Placement* are marked \checkmark .

As can be seen from Table 8, our attack necessitates neither adversarial patches nor intricate shape modifications as in the previous works. Hence, we do not have concerns regarding the printability of adversarial objects. Moreover, our attack operates as a black box attack, making it applicable to a broader range of situations. While LiDAR Seg [46] and ADS-DoS [45] share similar prerequisites with TrashFuzz, LiDAR Seg focuses on deceiving the LiDAR detection algorithm without considering the camera detection algorithm and ADS-DoS is a grey-box attack which requires knowledge of the planning module of the ADS. In contrast, TrashFuzz takes the entire perception system into consideration and is a black box attack. In summary, when compared to existing attacks, it can be concluded that TrashFuzz is relatively easy to conduct.

Threats to Validity. Given the nature of simulation-based testing, it is important to acknowledge the presence of potential validity threats to the identified issues. For instance, the ADS consumes a substantial amount of computational resources, and limitations in computational resources can introduce latency into the ADS. To address this challenge, we employ a solution by running the ADS and simulator on two separate machines connected by an Ethernet cable. During the experiment, we ensure memory cleanliness and exclude any concurrent tasks. As a result, we consistently achieve an average latency of less than 0.1 seconds for all the Apollo modules during simulations. Furthermore, we replicate the identification of issues at least three times to ensure that these issues are not the result of random latency. Despite taking these measures, in general, we cannot definitively rule out the possibility that a discovered issue might be influenced by the running environment. Nevertheless, identifying such problems remains valuable for enhancing the overall system.

5 RELATED WORK

Attacks for AV. ADSs are complex and security-critical systems, but ensuring their resilience against attacks is difficult. Two categories of works have introduced several attacks to analyse security issues of the ADS, which we review below.

The first category of research focuses on attacking the ADS *based on adversarial patches*. In several attacks [23], [24], [25], patches have been strategically placed on roadside billboards to influence the behaviour of the ADS. In another, a simple flat dirty patch on the road surface can disrupt the Automated Lane Centering of an ADS, causing it to deviate from the intended steering angle [14]. Similarly, the presence of an adversarial patch on a vehicle in front can interfere with the depth estimation algorithm of the ADS, potentially leading to collisions [15]. Finally, the use of projectors to create ‘shadows’ can introduce errors into the segmentation algorithm of the ADS, causing deviations in the bounding box of detected objects from the ground truth [16].

The second category of attacks explores how to attack ADSs *based on the placement of objects*. For example, MAF-ADV [11] manipulates the shape of an object, such as a traffic cone, making it invisible to both cameras and LiDAR object detection algorithms. Then, the attacker can place the adversarial object in front of the ADS to cause a collision. In the research by Zhu et al. [13], [46], objects such as cardboard, road signs, or commercial drones are strategically positioned at specific locations to reflect laser beams, generating misleading points that disrupt the LiDAR object detection and segmentation algorithms. The frustum attack [12] exploits the camera’s blind spots, utilising these regions to influence the LiDAR segmentation algorithm and consequently affecting the fusion of camera and LiDAR results. Wan et al. [45] strategically place objects such as traffic cones to provoke overly conservative behaviour within the planning module of the ADS. Furthermore, unconventional ‘objects’ like invisible lights are employed to disrupt the camera perception [47].

The aforementioned attacks rely on conspicuous patches or objects with non-standard shapes. Additionally, these adversarial attacks are mainly white-box attacks, which may be unrealistic in practice. With TrashFuzz, we present a black box attack that has the capability to induce hesitation or trigger aggressive driving behaviour in a state-of-the-art ADS Apollo. Furthermore, these behaviours can be induced by placements of objects that satisfy guidelines for road design.

Critical Scenario Generation. A number of works explore the safety and efficiency issues of ADS by generating critical scenarios. Part of these scenario-generation approaches centre around altering the behaviour of background vehicles to cause collisions. For instance, AVFuzzer [48] and DoppelTest [49] employ a genetic algorithm-based fuzzing engine to optimise scenarios, primarily focusing on minimizing the distance from other background vehicles. Similarly, AutoFuzz [50] proposes a constrained neural network evolutionary search approach to guide AVs into scenarios resulting in collisions or veering off the road. NADE [34] initially generates scenarios mimicking the natural driving behaviour of background vehicles but introduces deviations in their driving behaviour at key points to create adversarial scenarios likely to lead to collisions. CRISCO [51] assigns participants to execute impactful behaviors aimed at challenging the ADS, ultimately leading to collisions involving AVs. AVUnit [52] introduces a scenario description language that characterises the driving behaviour of background vehicles, pedestrians, and weather conditions,

TABLE 8: Prerequisites for applying different attacks

Methods	TrashFuzz (Ours)	MSF [11]	ADSDoS [45]	DeepBillboard [23]	Dirty Road [14]	Car Patch [15]	Frustum [12]	AttackZone [16]
Patch?	×	×	×	✓	✓	✓	×	✓
Shape?	×	✓	×	×	×	×	×	×
Placement?	✓	✓	✓	✓	✓	✓	✓	✓
Special?	×	×	×	×	×	×	✓	✓
White-B?	×	✓	×	✓	✓	✓	×	✓
Grey-B?	×	×	✓	×	×	×	×	×
Black-B?	✓	×	×	×	×	×	✓	×

proposing a fuzzing algorithm based on encoding scenarios described in this language. DeepCollision [53] employs a Reinforcement Learning algorithm to manipulate the driving environment, directing AVs toward collision scenarios. MOSAT [54] uses a multi-objective genetic algorithm to search for scenarios that cause collisions. Similarly, Rule-based Searching [55], Evolutionary-Algorithm-based Generation [56], and CMTS [57] all manipulate the driving behaviours of background vehicles to induce collision scenarios.

In addition to collision avoidance, more elaborate optimisation objectives have been explored as well. Law-Breaker [17] uses traffic laws as specifications and presents a coverage-based fuzzing algorithm to trigger various traffic law violations by modifying the driving behaviours of background vehicles. ABLE [58] employs active learning to efficiently extend the coverage of traffic laws. TARGET [59] uses GPT-3 to analyse traffic laws, thereby enabling the formulation of specifications for generating test scenarios. Althoff et al. [60] aim to minimise the passable area by modifying the driving behaviours of background vehicles. Metamorphic Testing of Driverless Cars [61] focuses on checking the relationships between the inputs and outputs across multiple executions of the ADS. The Baidu Group introduces a coverage-based feedback mechanism in their work [62], where the criterion is the extent of coverage of the driving area on the map. In other words, achieving a broader coverage of the driving area signifies a more favourable scenario. Hauer et al. [63] investigate the automated and manual modification of the driving behaviours of the background vehicles to cover all categories, framing this task as a Coupon Collector’s problem. MORLOT [64] proposes a method of many-Objective Reinforcement Learning for Online Testing of ADS, guiding AVs to violate 11 safety metrics, e.g. red light and collision infractions.

These works, however, primarily concentrate on mutating the driving behaviour of background vehicles, often overlooking the impact of object placements on ADS behaviour due to their unique perception systems. In this work, we investigate the influence of roadside objects on ADS, revealing that these objects can also significantly affect ADS driving behaviour, even when their placement follows the road design guidelines that characterise our natural scenarios.

6 CONCLUSION

In this paper, we introduced TrashFuzz, the first black box ADS testing approach based on generating natural (patch-free) adversarial scenarios that respect regulatory and company guidelines for the placement of roadside objects. Our approach utilises a greedy gradient-based fuzzing algorithm

that places these objects so as to exploit vulnerabilities in the ADS’s perception system and induce traffic law violations. We implemented TrashFuzz for the Apollo ADS and LGSVL simulator, and assembled an extensive library of everyday roadside objects using assets from the Unity Asset Store. We found that our approach could uncover natural scenarios that induced Apollo to violate 15 different Chinese traffic laws, including one in which an otherwise benign placement of bins overloaded Apollo’s perception system and caused it to misperceive an adjacent traffic light as green. These results highlight a current lack of resilience in a key ADS, and perhaps suggest guidelines for the placement of roadside objects may need to take into account the presence of AVs on the road. For example, regulating the shape and size of roadside trash bins may help prevent misclassifications, ensuring they are not mistaken for pedestrians or vehicles from any angle.

REFERENCES

- [1] S. O.-R. A. V. S. Committee *et al.*, “Taxonomy and definitions for terms related to driving automation systems for on-road motor vehicles,” *SAE International: Warrendale, PA, USA*, 2018.
- [2] Waymo. (2023) Waymo Driver. <https://waymo.com/waymo-driver/>. Online; accessed September 2024.
- [3] Baidu. (2023) Apollo. <https://www.apollo.auto/>. Online; accessed September 2024.
- [4] TuSimple. (2023) Autonomous driving technology designed for trucks. <https://www.tusimple.com/technology/>. Online; accessed September 2024.
- [5] Land Transport Authority. (2018) Code of practice for works on public streets 1. https://www.lta.gov.sg/content/dam/ltagov/industry_innovations/industry_matters/development_construction_resources/Street_Work_Proposals/codes_of_practice/COP_for_Works_on_Public_Streets_Sep2018Ed.pdf. Online; accessed September 2024.
- [6] Singapore Government. (2021) Street works (works on public streets) regulations. <https://sso.agc.gov.sg/SL/SWA1995-RG2>. Online; accessed September 2024.
- [7] National Park. (2019) Guidelines on greenery provision and tree conservation for developments. https://www.nparks.gov.sg/-/media/nparks-real-content/partner-us/nparks-handbook_version-4.pdf. Online; accessed September 2024.
- [8] Homewood Disposal Service. (2021) How to place your cart at the curb. <https://mydisposal.com/how-to-place-your-garbage-cart-at-the-curb>. Online; accessed September 2024.
- [9] KIMBLE. (2019) Trash cart placement. <https://www.kimblecompanies.com/trash-cart-placement>. Online; accessed September 2024.
- [10] GRANGER WASTE SERVICES. (2019) Cart placement. <https://www.grangerwasteservices.com/wp-content/uploads/2021/09/Cart-Placement-Flyer-no-time.pdf>. Online; accessed September 2024.
- [11] Y. Cao, N. Wang, C. Xiao, D. Yang, J. Fang, R. Yang, Q. A. Chen, M. Liu, and B. Li, “Invisible for both camera and lidar: Security of multi-sensor fusion based perception in autonomous driving under physical-world attacks,” in *2021 IEEE Symposium on Security and Privacy (SP)*. IEEE, 2021, pp. 176–194.

- [12] R. S. Hallyburton, Y. Liu, Y. Cao, Z. M. Mao, and M. Pajic, "Security analysis of {Camera-LiDAR} fusion against {Black-Box} attacks on autonomous vehicles," in *31st USENIX Security Symposium (USENIX Security 22)*, 2022, pp. 1903–1920.
- [13] Y. Zhu, C. Miao, T. Zheng, F. Hajiaghajani, L. Su, and C. Qiao, "Can we use arbitrary objects to attack lidar perception in autonomous driving?" in *Proceedings of the 2021 ACM SIGSAC Conference on Computer and Communications Security*, 2021, pp. 1945–1960.
- [14] T. Sato, J. Shen, N. Wang, Y. Jia, X. Lin, and Q. A. Chen, "Dirty road can attack: Security of deep learning based automated lane centering under physical-world attack," in *Proceedings of the 30th USENIX Security Symposium (USENIX Security 21)*, 2021.
- [15] Z. Cheng, J. Liang, H. Choi, G. Tao, Z. Cao, D. Liu, and X. Zhang, "Physical attack on monocular depth estimation with optimal adversarial patches," in *Computer Vision—ECCV 2022: 17th European Conference, Tel Aviv, Israel, October 23–27, 2022, Proceedings, Part XXXVIII*. Springer, 2022, pp. 514–532.
- [16] R. Muller, Y. Man, Z. B. Celik, M. Li, and R. Gerdes, "Physical hijacking attacks against object trackers," in *Proceedings of the 2022 ACM SIGSAC Conference on Computer and Communications Security*, 2022, pp. 2309–2322.
- [17] Y. Sun, C. M. Poskitt, J. Sun, Y. Chen, and Z. Yang, "LawBreaker: An approach for specifying traffic laws and fuzzing autonomous vehicles," in *ASE*. ACM, 2022, pp. 62:1–62:12.
- [18] Baidu. (2022) Apollo 7.0. <https://github.com/ApolloAuto/apollo/releases/tag/v7.0.0>. Online; accessed September 2024.
- [19] G. Rong, B. H. Shin, H. Tabatabaee, Q. Lu, S. Lemke, M. Mozeiko, E. Boise, G. Uhm, M. Gerow, S. Mehta *et al.*, "LGSVL simulator: A high fidelity simulator for autonomous driving," in *2020 IEEE 23rd International Conference on Intelligent Transportation Systems (ITSC)*, 2020, pp. 1–6.
- [20] Unity. (2023) Unity store. <https://assetstore.unity.com/>. Online; accessed September 2024.
- [21] Baidu. (2023) Latest Apollo. <https://github.com/ApolloAuto/apollo>. Online; accessed September 2024.
- [22] Autoware.AI. (2023) Autoware.AI. www.autoware.ai/. Online; accessed September 2024.
- [23] H. Zhou, W. Li, Z. Kong, J. Guo, Y. Zhang, B. Yu, L. Zhang, and C. Liu, "Deepbillboard: Systematic physical-world testing of autonomous driving systems," in *Proceedings of the ACM/IEEE 42nd International Conference on Software Engineering*, 2020, pp. 347–358.
- [24] N. Patel, P. Krishnamurthy, S. Garg, and F. Khorrami, "Adaptive adversarial videos on roadside billboards: Dynamically modifying trajectories of autonomous vehicles," in *2019 IEEE/RSJ International Conference on Intelligent Robots and Systems (IROS)*. IEEE, 2019, pp. 5916–5921.
- [25] —, "Overriding autonomous driving systems using adaptive adversarial billboards," *IEEE Transactions on Intelligent Transportation Systems*, vol. 23, no. 8, pp. 11 386–11 396, 2021.
- [26] A. Kurakin, I. Goodfellow, and S. Bengio, "Adversarial machine learning at scale," *arXiv preprint arXiv:1611.01236*, 2016.
- [27] G. Hinton, O. Vinyals, and J. Dean, "Distilling the knowledge in a neural network," *arXiv preprint arXiv:1503.02531*, 2015.
- [28] N. Papernot, P. McDaniel, X. Wu, S. Jha, and A. Swami, "Distillation as a defense to adversarial perturbations against deep neural networks," in *2016 IEEE symposium on security and privacy (SP)*. IEEE, 2016, pp. 582–597.
- [29] P. Samangouei, M. Kabkab, and R. Chellappa, "Defense-gan: Protecting classifiers against adversarial attacks using generative models," *arXiv preprint arXiv:1805.06605*, 2018.
- [30] A. Chakraborty, M. Alam, V. Dey, A. Chattopadhyay, and D. Mukhopadhyay, "Adversarial attacks and defences: A survey," *arXiv preprint arXiv:1810.00069*, 2018.
- [31] —, "A survey on adversarial attacks and defences," *CAAI Transactions on Intelligence Technology*, vol. 6, no. 1, pp. 25–45, 2021.
- [32] Singapore Government. (2021) Street works act 1995. <https://sso.agc.gov.sg/Act/SWA1995#top>. Online; accessed September 2024.
- [33] O. Maler and D. Nickovic, "Monitoring temporal properties of continuous signals," in *Formal Techniques, Modelling and Analysis of Timed and Fault-Tolerant Systems*, 2004, pp. 152–166.
- [34] S. Feng, X. Yan, H. Sun, Y. Feng, and H. X. Liu, "Intelligent driving intelligence test for autonomous vehicles with naturalistic and adversarial environment," *Nature communications*, vol. 12, no. 1, p. 748, 2021.
- [35] Autoware. (2023) Awsim document. <https://tier4.github.io/AWSIM/>. Online; accessed September 2024.
- [36] Unity Real-Time Development Platform. (2023) Unity. <https://unity.com/>. Online; accessed September 2024.
- [37] Sun Yang. (2023) Our website. Online; accessed September 2024. [Online]. Available: <https://trashfuzz.github.io/>
- [38] J. V. Deshmukh, A. Donzé, S. Ghosh, X. Jin, G. Juniwal, and S. A. Seshia, "Robust online monitoring of signal temporal logic," *Formal Methods in System Design*, vol. 51, no. 1, pp. 5–30, 2017.
- [39] D. Ničković and T. Yamaguchi, "RTAMT: Online robustness monitors from STL," in *International Symposium on Automated Technology for Verification and Analysis*, 2020, pp. 564–571.
- [40] C. Baier and J.-P. Katoen, *Principles of model checking*. MIT press, 2008.
- [41] LGSVL. (2023) Cyberrt. <https://github.com/lgsvl/CyberRT>. Online; accessed September 2024.
- [42] Carla. (2023) Ros bridge for autoware and carla. <https://github.com/carla-simulator/carla-autoware>. Online; accessed September 2024.
- [43] S. Mirjalili, *Evolutionary Algorithms and Neural Networks - Theory and Applications*, ser. Studies in Computational Intelligence. Springer, 2019, vol. 780.
- [44] A. Dosovitskiy, G. Ros, F. Codevilla, A. M. López, and V. Koltun, "CARLA: an open urban driving simulator," in *CoRL*, ser. Proceedings of Machine Learning Research, vol. 78. PMLR, 2017, pp. 1–16.
- [45] Z. Wan, J. Shen, J. Chuang, X. Xia, J. Garcia, J. Ma, and Q. A. Chen, "Too afraid to drive: Systematic discovery of semantic dos vulnerability in autonomous driving planning under physical-world attacks," *arXiv preprint arXiv:2201.04610*, 2022.
- [46] Y. Zhu, C. Miao, F. Hajiaghajani, M. Huai, L. Su, and C. Qiao, "Adversarial attacks against lidar semantic segmentation in autonomous driving," in *Proceedings of the 19th ACM Conference on Embedded Networked Sensor Systems*, 2021, pp. 329–342.
- [47] W. Wang, Y. Yao, X. Liu, X. Li, P. Hao, and T. Zhu, "I can see the light: Attacks on autonomous vehicles using invisible lights," in *Proceedings of the 2021 ACM SIGSAC Conference on Computer and Communications Security*, 2021, pp. 1930–1944.
- [48] G. Li, Y. Li, S. Jha, T. Tsai, M. B. Sullivan, S. K. S. Hari, Z. Kalbarczyk, and R. K. Iyer, "AV-FUZZER: finding safety violations in autonomous driving systems," in *ISSRE*. IEEE, 2020, pp. 25–36.
- [49] Y. Huai, Y. Chen, S. Almanee, T. Ngo, X. Liao, Z. Wan, Q. A. Chen, and J. Garcia, "Doppelgänger test generation for revealing bugs in autonomous driving software," in *2023 IEEE/ACM 45th International Conference on Software Engineering (ICSE)*. IEEE, 2023, pp. 2591–2603.
- [50] Z. Zhong, G. Kaiser, and B. Ray, "Neural network guided evolutionary fuzzing for finding traffic violations of autonomous vehicles," *IEEE Transactions on Software Engineering*, 2022.
- [51] H. Tian, G. Wu, J. Yan, Y. Jiang, J. Wei, W. Chen, S. Li, and D. Ye, "Generating critical test scenarios for autonomous driving systems via influential behavior patterns," in *Proceedings of the 37th IEEE/ACM International Conference on Automated Software Engineering*, 2022, pp. 1–12.
- [52] Y. Zhou, Y. Sun, Y. Tang, Y. Chen, J. Sun, C. M. Poskitt, Y. Liu, and Z. Yang, "Specification-based autonomous driving system testing," *IEEE Transactions on Software Engineering*, vol. 49, no. 6, pp. 3391–3410, 2023.
- [53] C. Lu, Y. Shi, H. Zhang, M. Zhang, T. Wang, T. Yue, and S. Ali, "Learning configurations of operating environment of autonomous vehicles to maximize their collisions," *IEEE Transactions on Software Engineering*, vol. 49, no. 1, pp. 384–402, 2022.
- [54] H. Tian, Y. Jiang, G. Wu, J. Yan, J. Wei, W. Chen, S. Li, and D. Ye, "Mosat: finding safety violations of autonomous driving systems using multi-objective genetic algorithm," in *Proceedings of the 30th ACM Joint European Software Engineering Conference and Symposium on the Foundations of Software Engineering*, 2022, pp. 94–106.
- [55] S. Masuda, H. Nakamura, and K. Kajitani, "Rule-based searching for collision test cases of autonomous vehicles simulation," *IET Intell. Transp. Syst.*, vol. 12, no. 9, pp. 1088–1095, 2018.
- [56] M. Klischat and M. Althoff, "Generating critical test scenarios for automated vehicles with evolutionary algorithms," in *IV*. IEEE, 2019, pp. 2352–2358.
- [57] W. Ding, M. Xu, and D. Zhao, "CMTS: A conditional multiple trajectory synthesizer for generating safety-critical driving scenarios," in *ICRA*. IEEE, 2020, pp. 4314–4321.
- [58] X. Zhang, W. Zhao, Y. Sun, J. Sun, Y. Shen, X. Dong, and Z. Yang, "Testing automated driving systems by breaking many laws ef-

- ficiently," in *Proceedings of the 32nd ACM SIGSOFT International Symposium on Software Testing and Analysis*, 2023, pp. 942–953.
- [59] Y. Deng, J. Yao, Z. Tu, X. Zheng, M. Zhang, and T. Zhang, "Target: Traffic rule-based test generation for autonomous driving systems," *arXiv preprint arXiv:2305.06018*, 2023.
 - [60] M. Althoff and S. Lutz, "Automatic generation of safety-critical test scenarios for collision avoidance of road vehicles," in *Intelligent Vehicles Symposium*. IEEE, 2018, pp. 1326–1333.
 - [61] Z. Q. Zhou and L. Sun, "Metamorphic testing of driverless cars," *Communications of the ACM*, vol. 62, no. 3, pp. 61–67, 2019.
 - [62] Z. Hu, S. Guo, Z. Zhong, and K. Li, "Coverage-based scene fuzzing for virtual autonomous driving testing," *CoRR*, vol. abs/2106.00873, 2021.
 - [63] F. Hauer, T. Schmidt, B. Holzmüller, and A. Pretschner, "Did we test all scenarios for automated and autonomous driving systems?" in *ITSC*. IEEE, 2019, pp. 2950–2955.
 - [64] F. U. Haq, D. Shin, and L. C. Briand, "Many-objective reinforcement learning for online testing of dnn-enabled systems," in *2023 IEEE/ACM 45th International Conference on Software Engineering (ICSE)*. IEEE, 2023, pp. 1814–1826.